

Anomaly Detection in Road Networks using Sliding-Window Tensor Factorization

Ming Xu, Jianping Wu, Haohan Wang, Mengxin Cao, Dongmei Hu

Abstract—Anomaly detection on road networks can be used to sever for emergency response and is of great importance to traffic management. However, none of the existing approaches can deal with the diversity of anomaly types. In this paper, we propose a novel framework to detect multiple types of anomalies. The framework incorporates real-time and historical traffic into a tensor model and acquires spatial and different scale temporal pattern of traffic in unified model using tensor factorization. Furthermore, we propose a sliding window tensor factorization to improve the computational efficiency. Basing on this, we can identify different anomaly types through measuring the deviation from different spatial and temporal pattern. Then, to promote a deeper understanding of the detected anomalies, we use an optimization method to discover the path-level anomalies. The core idea is that the anomalous path inference is formulated as L1 inverse problem by considering the sparsity of anomalies and flow on paths simultaneously. We conduct synthetic experiments and real case studies based on a real-world dataset of taxi trajectories. Experiments verify that the proposed framework outperforms all baseline methods on efficiency and effectiveness, and the framework can provide a better understanding for anomalous events.

Index Terms—anomaly detection, tensor factorization, sliding window, L1 inverse problem

I. INTRODUCTION

THE sensing and understanding of traffic situation in road networks is of vital importance to transportation operators. In particular, an unusual event (anomaly), such as an accident, concert or football match, can cause traffic congestion that may diffuse rapidly. If an anomaly occurs, we need to detect it promptly and accurately for an emergency response. In general, an anomaly means a dramatic traffic change that does not follow the expected pattern. Therefore, a naïve solution is utilizing the statistical models to determine the threshold of normal traffic and detect anomalies on a single road segment or in a small area depending on whether the traffic volume

exceeds the threshold. However, a disadvantage of this method is that the threshold of each road segment needs to be determined separately due to the complexity of road characteristics, such as traffic capacity, geographical conditions and road quality. Thus, it is intractable to apply this method to a city-wide scale; In addition, this method cannot determine whether two anomalies have a relationship. To improve the effectiveness of detection, a family of methods based on statistical theory and machine learning are proposed. We will describe these methods in the “related work” section. However, these methods mainly focus on single type of anomaly, and the diversity of the anomalies in road network is not considered.

Fig. 1 presents a simple example of small road network including 4 nodes (A-D) and 5 directed edges during operational periods of 103 days. Each day is partitioned into 96 time intervals that are defined as 15 minutes. Each grid represents the traffic situation of the network during one time interval. For simplicity, we assume that the traffic change of each edge follows its own stable trend until day 101. However, the traffic trend of edge $B \rightarrow D$ shows a quite difference from other edges. We refer to edge $B \rightarrow D$ as the 1st anomaly type. In reality, this anomaly type may be the roads near some famous tourist attractions. These roads may have a great flow over the daytime unlike others with the morning or evening rush hour. In day 101, edge $B \rightarrow C$ shows a different traffic change compared with its own historical trend and other edges. This type may be caused by an accident or temporary traffic restriction. The 3rd anomaly type emerges during day 102. As we can see, majority edges show similar traffic changes that do not follow their historical pattern. This anomaly type can be analogous to the citywide crowd event with an impact on large scale traffic. In terms of day 103, it has a slightly difference from historical pattern in the whole network, so it is regarded as a normal day.

The fundamental differences among these anomaly types are determined by the characteristics of traffic flow listed as follow

- Spatial correlation. The following road segments are likely to have similar traffic pattern: 1) the road segments close to each other; 2) the road segments connected regions that have similar social functions, such as residential region and working place;
- Short-term correlation. Observing from a short-term scale, the traffic flow may fluctuate greatly. However, the traffic volumes in close propinquity to each other usually have dependencies.
- Long-term correlation. The traffic change trend is regular

Ming Xu is with the Department of Civil Engineering, Tsinghua University, Beijing, 100084, China (e-mail: mxu@tsinghua.edu.cn).

Jianping Wu is with the Department of Civil Engineering, Tsinghua University, Beijing, 100084, China (e-mail: jianpingwu@tsinghua.edu.cn).

Haohan Wang is with the School of Computer Science, Carnegie Mellon University, Pittsburgh PA, 15213, USA (e-mail: haohanw@andrew.cmu.edu).

Mengxin Cao is with the Department of Internet of Things Engineering, Beijing University of Posts and Telecommunications, Beijing, 100876, China (e-mail: caomengxin@bupt.edu.cn).

Dongmei Hu is with the Department of Civil Engineering, Tsinghua University, Beijing, 100084, China (e-mail: hudm13@tsinghua.edu.cn).

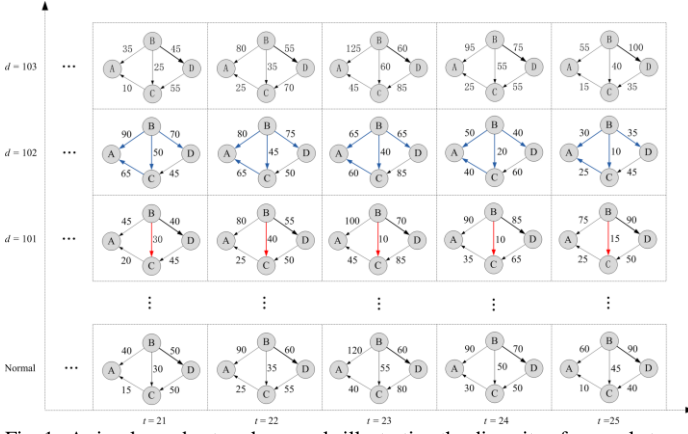


Fig. 1. A simple road network example illustrating the diversity of anomaly types

and stable from a long-term (week scale or month scale) perspective. Specifically, the traffic flow usually shows periodic variation.

The 1st and 2nd anomaly types are link-level. The 1st anomaly obeys the long-term correlation but breaks the short-term correlation; the 2nd type breaks both the short-term and long-term correlations; the 3rd type can be detected from a day dimension perspective, and it breaks both the short-term and the spatial correlations. Detection of all these types of anomalies using one model is very challenging. For it requires us to capture traffic trend considering both the spatial dimension and different scales temporal dimensions simultaneously.

To tackle this challenge, we propose a novel anomaly detection framework that monitors the traffic of road networks through real-time trajectory data of massive vehicles. In this framework, we represent the traffic of road network as a three order tensor and utilize tensor factorization to simultaneously discover spatial pattern and different scale temporal pattern in unified model. For online applications, we propose a sliding window tensor factorization method (SWTD) to improve computational efficiency. In each turn, this method needn't recalculate the entire tensor, that is, only the updated data is considered to integrating into the previous result. Through tensor factorization, we obtain three factor matrices representing subspace of each dimension and one core tensor capturing the trend of traffic change. Then we determine whether a certain anomaly type occurs according to deviation from the normal traffic trend of the corresponding dimensions. Furthermore, we propose an anomalous paths inference method to provide a better understanding according to the link-level anomalies.. Differing from method in [1] that only considers sparsity of anomaly, our method combines sparsity of anomaly and flow on paths. Finally, we conduct a synthetic experiment and a real case study based on a real-world trajectory dataset of massive taxicabs. Experiments evaluate the effectiveness and efficiency of the proposed framework.

II. PRELIMINARIES

A. Tensor concepts

A tensor is a multi-dimensional (multi-way or multi-mode) array or a multidimensional matrix. The order of tensor is

number of dimensions. In particular, an n th order ($n \geq 3$) tensor can be imaged as a hypercube of data, and scalar, vector and matrix can also be regarded as special forms of tensors, which are respectively 0th, 1st and 2nd order tensors..

B. Tensor Factorization

To guarantee to information integrity, the data from applications in many fields, such as telecommunications, transportations, social networks, e-commerce, environmental science, biology, etc., can be naturally represented by tensors. However, based on this data representation, how to discover the implicit structures and internal relationships of tensor data is our principal concern. A simple method is to unfold the tensor to a large matrix along a certain dimension, then analysis it using the subspace technologies, such as PCA or NMF. But this method separates the links between different dimensions, and loses some important implicit structures.

For singular value decomposition (SVD), given an arbitrary matrix $X \in \mathbb{R}^{I_1 \times I_2}$, there must be $X = USV^T$, where $U \in \mathbb{R}^{I_1 \times I_1}$, $V \in \mathbb{R}^{I_2 \times I_2}$ are orthogonal matrixes; $S \in \mathbb{R}^{I_1 \times I_2}$ is pseudo-diagonal matrix. If referring to X as a 2nd order tensor, its SVD can be also written as $X = S \times_1 U \times_2 V$ according to n-mode product of a tensor. For higher order tensors, the diagonalization and orthogonally cannot be guaranteed simultaneously. And emphasizing on different aspects can obtain different forms of decomposition. The two basic methods are 1) CANDECOMP/PARAFAC (CP) decomposition that preserves the diagonal form, and 2) Tucker decomposition that emphasizes the orthogonally [2]. The CP decomposition factorizes a tensor into a sum of R component rank-one tensors, where R is the rank of the tensor. For example, a 3rd order tensor $X \in \mathbb{R}^{I_1 \times I_2 \times I_3}$ can be factorized as follow

$$X = \sum_{r=1}^R a_r \circ b_r \circ c_r \quad (1)$$

where the symbol “ \circ ” represents the vector outer product. This means that each element of the tensor is the product of the corresponding vector elements $a_r \in \mathbb{R}^{I_1}$, $b_r \in \mathbb{R}^{I_2}$ and $c_r \in \mathbb{R}^{I_3}$, for $r = 1, \dots, R$.

Tucker factorizes a tensor into a core tensor multiplied by a matrix along each mode. For example, Tucker factorizes χ as follow

$$X = G \times_1 U_1 \times_2 U_2 \times_3 U_3 \quad (2)$$

where G is the core tensor; U_i is the i -mode factor matrix. The typical tucker decompositions are Tucker1 (higher order SVD) and Tucker3 (HOOI), and the nature of Tucker is the multiple linear extension of SVD on multi-mode.

III. METHODOLOGIES

A. Framework

As demonstrated in Fig. 2, our framework can be divided into two parts, information extraction and anomaly detection.

Information extraction: Our framework receives real-time trajectory data stream generated by massive vehicles equipped

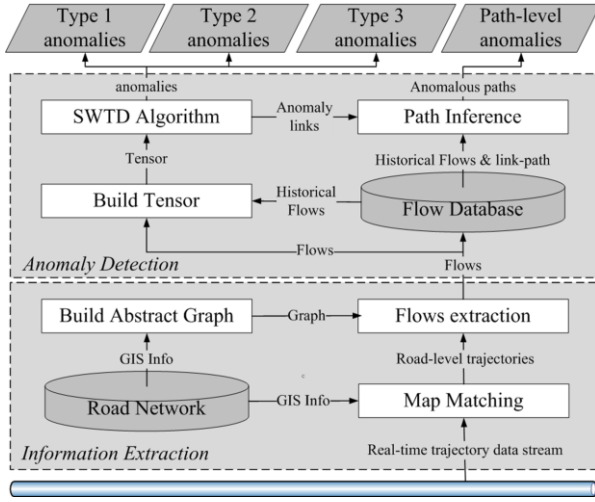


Fig. 2. Framework of the proposed method for anomaly detection

GPS device. The original trajectory data of each vehicle consists of its geospatial coordinate readings (longitude and latitude) with the sampling timestamps. However, due to the noise in the GPS samples, the readings often deviate from the actual road segments. Therefore, we use the map matching algorithm [3] to map each GPS reading onto the corresponding road segment. In addition, we build an abstract graph based on the road network. To this end, we use the algorithm [4] to partition the urban map into non-overlapping regions. Such a partition algorithm preserve the semantic meaning of a region, e.g., schools, parks, business areas, residential areas, etc. Then, an abstract graph is constructed. As Fig. 3 presented, each region is regarded as a node of the graph, and any two adjacent regions have a link. Note that one link may refer to multiple road segments. Based on these, we recalculate flows on the graph. Considering the abstract graph as the analysis object instead of original road network enables our model to discover more meaningful and influential events.

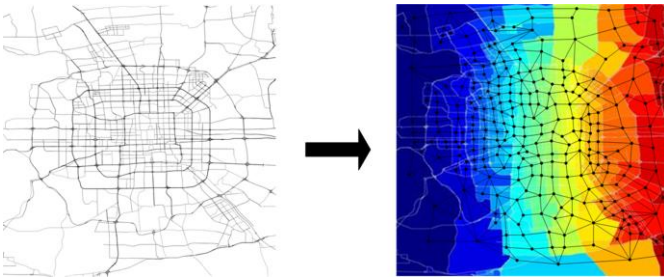


Fig. 3. Abstract graph of the road network

Anomaly detection: We represent traffic of the road network as a tensor described in detail later. The tensor consists of current traffic data and historical traffic data. The core of this framework is SWTD, which is an online tensor factorization algorithm for detecting different anomaly types. Finally, we use an optimization technology to infer the anomalous paths according to anomalous links discovered by SWTD. The path-level anomaly information is more valuable to traffic control and guidance, for it often reveals the cause of the anomaly and help the transportation managers understand impact scope of the events

B. Data Model

Like application data from many other fields, the traffic data in the road network are suitably described as a tensor and can be represented as many forms. Here, we construct a traffic 3rd order tensor $X \in \mathbb{R}^{I_1 \times I_2 \times I_3}$ with modes of link \times time \times day, as demonstrated in Fig. 4. Specifically, we partition the urban map into a collection of non-overlapping regions, and it can be considered that there is a bidirectional link between any two adjacent regions. In the traffic tensor, an element $x_{i_1 i_2 i_3}$ represents the traffic volume of link l_{i_1} at time interval t_{i_2} in day d_{i_3} ; I_1 is the total number of links in the road network;. Actually, due to the dynamic growth of traffic data, the scales of time dimension and day dimension are increasing. To deal with such stream data efficiently, we respectively set a sliding window on time and day dimension. I_2 and I_3 are the size of the sliding window on time and day dimension respectively; t_{I_2-1} denotes the current time interval; d_{I_3-1} denotes the current day. When the new data arrives, remove the elements $X_{:,0,:}$ of time dimension indexed by “0”, $X_{:,(I_2-1),:}$ represents the new part of data, and $X_{:,(I_2-1),(I_3-1)}$ is the data of current time in current day and can be collected online, and the elements $X_{:,(I_2-1),0} \sim X_{:,(I_2-1),(I_3-2)}$ at current time of previous day can be retrieved from archived data.

C. Sliding window tensor factorization

In this subsection, we use the tucker factorization to obtain one core tensor Ω and three factor matrices $W^{(1)} \in \mathbb{R}^{I_1 \times R_1}$, $W^{(2)} \in \mathbb{R}^{I_2 \times R_2}$, and $W^{(3)} \in \mathbb{R}^{I_3 \times R_3}$. The core tensor reflects the traffic change trend simultaneously considering the space, time and day dimensions. The factor matrices represent the orthogonal subspaces that capture the traffic change trend in their respective dimensions. Specifically, we use the HOOI algorithm that considers interactions among the dimensions when optimizing for each dimension. HOOI uses the alternating least squares method to complete the multi-dimensions approximation of the origin tensor, and its objective is to minimize the reconstruction error e given as.

$$e = \left\| X - X \prod_{l=1}^3 W^{(l)} (W^{(l)})^T \right\|_F^2 \quad (3)$$

However, HOOI requires inputting all tensor data at one time, and its iterative mode has very high time and space cost. Therefore, it is only used for the cold start of our method. For the traffic tensor updated dramatically, we propose SWTD. SWTD learns an online low dimension tensor subspace based on the original core tensor, removed elements and new arrived elements. Before describing SWTD, we first introduce the Improved Fast Approximate Subspace Tracking algorithm (IFAST) [5] invoked in SWTD. IFAST can factorize a sliding window matrix with a low cost liking SVD. Specifically, given a sequence S consisting of length n column vectors, the maximum length of S is m . Suppose that k vectors in this sequence are updated at each time step. At time steps t and $t+1$, two matrices $S_{t-1} = [s_{t-m} \ s_{t-m+1} \ \dots \ s_{t-1}]$ and $S_t =$

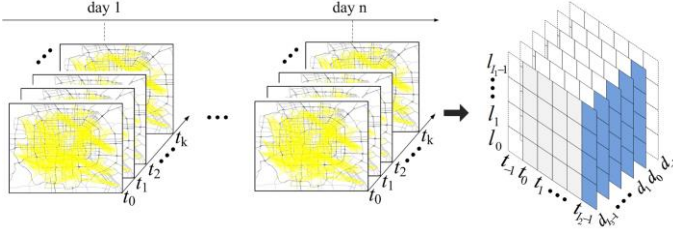


Fig. 4. The 3rd order sliding window tensor of traffic in the road network

$[s_{t-m+k} \ s_{t-m+1+k} \ \dots \ s_{t-1+k}]$ can be obtained respectively. Let \sum_{t-1} denotes the top r largest singular values of S_{t-1} and W_{t-1} denotes the left singular vector corresponding to \sum_{t-1} . The goal is to calculate \sum_t and W_t at a low cost without re-performing SVD on S_t . To achieve this, IFAST forms an approximate matrix F with size of $(r + 2k) \times (r + 2k)$ for S_t , which contains all the valid information for calculating the left singular vector and singular value of S_t . Thus, the singular value of F can be regard as a good approximation to that of S_t . Due to $(r + 2k) \times (r + 2k) \ll m \times n$, the SVD on F performs much faster compared with S_t . Next, we describe how to use IFAST for sliding window tensor decomposition. Let us consider updating a 3rd order sliding window tensor $X_{t-1} \in \mathbb{R}^{I_1 \times I_2 \times I_3}$ at time step $t-1$. When new data $B_t \in \mathbb{R}^{I_1 \times I_2 \times I_3}$ arrives at time step t , the old data $A_t \in \mathbb{R}^{I_1 \times I_2 \times I_3}$ is removed from X_{t-1} . X_t is represented as follow

$$X_t = [A_t \downarrow_2 X_{t-1} \uparrow_2 B_t] \quad (4)$$

where the operation “ \downarrow_2 ” removes the left part from the right tensor along the 2nd order (time dimension); the operation “ \uparrow_2 ” merges the left tensor and right part along the 2nd order. Fig. 5 demonstrates the process of unfolding A_t and the relations among the current unfolding matrices along each mode $X_t^{(1)} \in \mathbb{R}^{I_1 \times (I_2 \times I_3)}$, $X_t^{(2)} \in \mathbb{R}^{I_2 \times (I_3 \times I_1)}$, $X_t^{(3)} \in \mathbb{R}^{I_3 \times (I_1 \times I_2)}$, the previous unfolding matrices $X_{t-1}^{(1)} \in \mathbb{R}^{I_1 \times (I_2 \times I_3)}$, $X_{t-1}^{(2)} \in \mathbb{R}^{I_2 \times (I_3 \times I_1)}$, $X_{t-1}^{(3)} \in \mathbb{R}^{I_3 \times (I_1 \times I_2)}$, the newly arrived matrices $B_t^{(1)} \in \mathbb{R}^{I_1 \times (I_3 \times I_1)}$, $B_t^{(2)} \in \mathbb{R}^{I_2 \times (I_3 \times I_1)}$, $B_t^{(3)} \in \mathbb{R}^{I_3 \times (I_1 \times I_2)}$ and the removed matrices $A_t^{(1)} \in \mathbb{R}^{I_1 \times (I_3 \times I_1)}$, $A_t^{(2)} \in \mathbb{R}^{I_2 \times (I_3 \times I_1)}$, $A_t^{(3)} \in \mathbb{R}^{I_3 \times (I_1 \times I_2)}$. As showed in Fig. 3, the unfolding matrices along mode 1 and mode 3 are updated in the column vector space. In particular, $X_{t-1}^{(1)}$ is represented as $X_{t-1}^{(1)} = [A_{t-1}^{(1)} \downarrow_1 X_{t-1}^{(1)} \uparrow_1 B_{t-1}^{(1)}]$, and its SVD can be directly obtained using IFAST. However, with respect to $X_{t-1}^{(3)}$, it can be obtained through column exchange and transpose on $[A_{t-1}^{(3)} \downarrow_3 X_{t-1}^{(3)} \uparrow_3 B_{t-1}^{(3)}]$. To achieve this, we introduce an identity matrix U with rank $(I_2 + 1)I_1$ as follow

$$U = [H_1 \uparrow E_1 \uparrow Q_1 \uparrow H_2 \uparrow E_2 \uparrow Q_2 \uparrow \dots H_{I_1} \uparrow E_{I_1} \uparrow Q_{I_1}] \quad (5)$$

where H_i corresponds to the Dashed regions; E_i corresponds to the white regions; Q_i corresponds to the blue regions. Then we define a counterchange matrix P obtained by column exchange and transpose on U and formulated as follow

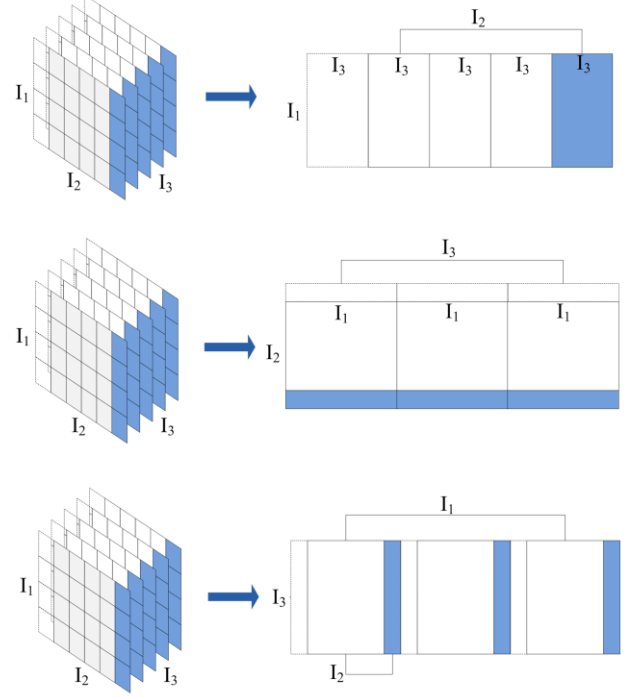


Fig. 5. Illustration of unfolding a 3rd order traffic tensor

$$P = [H_1 \uparrow \dots \uparrow H_{I_1} \uparrow E_1 \uparrow \dots \uparrow E_{I_1} \uparrow Q_1 \uparrow \dots \uparrow Q_{I_1}]^T \quad (6)$$

Next, $X_t^{(3)}$ can be obtained by $X_t^{(3)} = [A_t^{(3)} \downarrow_3 X_{t-1}^{(3)} \uparrow_3 B_t^{(3)}] \cdot P$, and we can also perform IFAST on $X_t^{(3)}$ to calculate its SVD. The mode-2 unfolding matrix $X_t^{(2)}$ is updated in row subspace, and it is formulated as.

$$X_t^{(2)} = \left[[A_t^{(2)}]^T \downarrow [X_{t-1}^{(2)}]^T \uparrow [B_t^{(2)}]^T \right]^T \quad (7)$$

Note that we need to perform IFAST on the transpose of $X_t^{(2)}$ to obtain its SVD, and then choose the right singular vector to calculate the factor matrix of time dimension. More details are presented in Algorithm 1.

D. Anomaly Detection

Tensor factorization is advanced subspace embedding technology for anomaly detection derived from matrix-based dimensionality reduction solutions, such as PCA. The idea of such methods is that data can be projection onto a low dimension subspace that the difference between the normal samples and anomalies are further magnified. With respect to each factor matrix, the column eigenvectors corresponding to the largest eigenvalues capture most significant information of origin tensor along its dimension, and anomalies possibly locate in the subspace formed by remaining smaller eigenvectors. Therefore, different anomaly types can be identified through simultaneously examining residual subspace of different factor matrixes. Specifically, to detect the first and second anomaly type, for each link, we need to check the traffic changes in a few continue time intervals from a historical

ALGORITHM I

SLIDING WINDOW TENSOR FACTORIZATION

Input: new tensor elements $B_t \in \mathbb{R}^{I_1 \times I_2 \times 1}$, removed tensor elements $A_t \in \mathbb{R}^{I_1 \times I_2 \times 1}$, old factor matrix $W_{t-1}^{(1)} \in \mathbb{R}^{I_1 \times R_1}$, $W_{t-1}^{(2)} \in \mathbb{R}^{I_2 \times R_2}$, $W_{t-1}^{(3)} \in \mathbb{R}^{I_3 \times R_3}$

Output: core tensor $\Omega_t \in \mathbb{R}^{I_1 \times I_2 \times I_3}$, new matrix $W_t^{(1)} \in \mathbb{R}^{I_1 \times R_1}$, $W_t^{(2)} \in \mathbb{R}^{I_2 \times R_2}$, $W_t^{(3)} \in \mathbb{R}^{I_3 \times R_3}$

- 1 Mode-1 unfold X_t as $X_{t-1}^{(1)}$
- 2 Mode-1 unfold A_t as $A_t^{(1)}$
- 3 Mode-1 unfold B_t as $B_t^{(1)}$
- 4 Form $X_t^{(1)} = [A_t^{(1)} \downarrow_2 X_{t-1}^{(1)} \uparrow_2 B_t^{(1)}]$
- 5 Use IFAST for $(W_t^{(1)}, \Sigma_t^{(1)}) = \text{IFAST_SVD}(X_t^{(1)}, W_{t-1}^{(1)}, \Sigma_{t-1}^{(1)})$
- 6 Mode-3 unfold X_t as $X_{t-1}^{(3)}$
- 7 Mode-3 unfold A_t as $A_t^{(3)}$
- 8 Mode-3 unfold B_t as $B_t^{(3)}$
- 9 Form $X_t^{(3)} = [A_t^{(3)} \downarrow_3 X_{t-1}^{(3)} \uparrow_3 B_t^{(3)}] \cdot P$
- 10 Use IFAST for $(W_t^{(2)}, \Sigma_t^{(2)}) = \text{IFAST_SVD}(X_t^{(2)}, W_{t-1}^{(2)}, \Sigma_{t-1}^{(2)})$
- 11 Mode-2 unfold X_t as $X_{t-1}^{(2)}$
- 12 Mode-2 unfold A_t as $A_t^{(2)}$
- 13 Mode-2 unfold B_t as $B_t^{(2)}$
- 14 Form $X_t^{(2)} = [[A_t^{(2)}]^T \downarrow [X_{t-1}^{(2)}]^T \uparrow [B_t^{(2)}]^T]^T$
- 15 Use IFAST for $(\hat{W}_t^{(3)}, \hat{\Sigma}_t^{(3)}) = \text{IFAST_SVD}([X_t^{(3)}]^T, W_{t-1}^{(3)}, \Sigma_{t-1}^{(3)})$
- 16 $W_t^{(3)} = \hat{W}_t^{(3)} = X_t^{(3)} \hat{\Sigma}_t^{(3)-1}$
- 17 Calculate the core tensor $\Omega_t = X_t \times_1 W_t^{(1)} \times_2 W_t^{(2)} \times_3 W_t^{(3)}$

perspective, as well as the traffic changes in different days from a short-term time series perspective. First, the traffic $\bar{X}_t^{(2)}$ on normal subspace of time dimension can be calculated as $\bar{X}_t^{(2)} = X_t \times_2 W_t^{(2)} (W_t^{(2)})^T$, and the traffic component $\tilde{X}_t^{(2)}$ on the anomaly subspace of time dimension can be calculated as $\tilde{X}_t^{(2)} = X_t \times_2 (I - W_t^{(2)} (W_t^{(2)})^T)$. Similarly, the traffic component $\tilde{X}_t^{(3)}$ on the anomaly subspace of day dimension is calculated as $\tilde{X}_t^{(3)} = X_t \times_3 (I - W_t^{(3)} (W_t^{(3)})^T)$. Then link i is considered as an anomalous link of the 1st type, when $\|vec((\tilde{X}_t^{(2)})_{i::})\|^2 > \delta_2$ and $\|vec((\tilde{X}_t^{(3)})_{i::})\|^2 < \delta_3$ simultaneously, where $vec(X)$ denotes the vectorization of tensor X ; δ_2 and δ_3 are the threshold determined by Q-statistic [6]. If $\|(\tilde{X}_t^{(2)})_{i:(I_3-1)}\|^2 > \delta_2$ and $\|(\tilde{X}_t^{(3)})_{i:(I_3-1)}\|^2 > \delta_3$ are met simultaneously, i will be considered as the 2nd anomaly type. The detection of the 3rd anomaly type is in respect of each day. And the anomaly traffic component on spatial dimension is captured using $\tilde{X}_t^{(1)} = X_t \times_1 (I - W_t^{(1)} (W_t^{(1)})^T)$. The conditions for judgment of the third anomaly type are $\|vec((\tilde{X}_t^{(1)})_{(I_1-1)::})\|^2 > \delta_1$ and $\|vec((\tilde{X}_t^{(2)})_{(I_1-1)::})\|^2 > \delta_2$.

E. Inferring routes accountable for anomalies

In this subsection, we infer the paths accountable for anomalous link after anomaly detection phase. The analogous studies [7] are emerged in the field of IP network traffic monitoring. Their core idea is to formulate the inference of OD flow anomalies as an under-constrained linear programming problem and introduce the assumption of anomaly sparsity to search the solution. The study [1] is the first to apply a similar

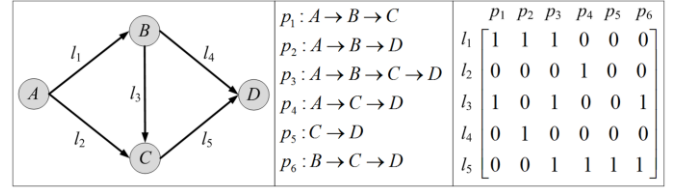


Fig. 6. An example of the proposed method for anomaly detection

method in the road network. In this research, a link-path binary matrix $A \in \mathbb{R}^{m \times n}$ representing the relationship between m links and n paths is constructed through extracting information from trajectories of vehicles. If link i is on the path j , $A_{ij} = 1$, otherwise, $A_{ij} = 0$. And the binary vector $b \in \mathbb{R}^m$ denotes the states of m links obtained in anomaly detection phase. If link i is anomalous, $b_i = 1$, otherwise $b_i = 0$; the vector $x \in \mathbb{R}^n$ denotes the states of n paths to infer. Given these, the relationship between state of links and paths can be represented as $Ax=b$. This is a typical ill-posed problem, since the paths substantially outnumber the links. To solve this, a constraint condition that assumes the sparsity of anomaly is increased. Then the L1 norm technology is used to obtain the sparse solution. In our research, we find that this method may have no solution, due to the great strictness of $Ax = b$. Therefore, we modify it as $Ax-b \geq 0$, and formulate the problem as finding the best matched paths of anomalous links:

$$\text{minimize } \|Ax - b\|_1 \text{ s.t. } Ax - b \geq 0, x \geq 0 \quad (8)$$

However, we find it still has the potential to improve. Because flow on paths is ignored, despite it is an important factor. Intuitively, a greater flow is more likely to cause anomalies. Therefore, we improve the previous method through a trade-off between the sparsity of anomaly and flow on paths. Specifically, we formulate it as the following

$$\text{minimize } \|x \cdot v^{-1}\|_1 \text{ s.t. } Ax - b \geq 0, x \geq 0 \quad (9)$$

where $v \in \mathbb{R}^n$ denotes flow matrix of paths, which can be obtained; the vectors v^{-1} denotes the operation that replaces each element of vector v with its reciprocal. Fig. 6 gives a simple network example, its topology, paths and the corresponding link-path matrix A are shown in Fig. 6(a), (b) and (c). Suppose that l_3 is an anomalous link, i.e. $b = [0, 0, 1, 0, 0]^T$, and we obtain $v = [10, 5, 15, 10, 20, 45]^T$ retrieval from flow database. In our inference method, the solution of formula (9) is $x = [0, 0, 0, 0, 0, 1]^T$, it indicates that p_6 is closely related to the anomaly. This is reasonable, because p_6 has a great flow, and its flow change is likely to cause the anomaly; while the solution of (8) is $x = [0.5, 0, 0, 0, 0, 0.5]^T$, for both of p_5 and p_6 are the best matched paths of l_3 . Whereas if the sparsity is only considered, $x = [0.3, 0, 0.4, 0, 0, 0.3]^T$. That means, this solution is inclined to pick out all the paths passed through the anomalous link, however, p_1 and p_3 both have a small flow and are unlikely accountable for the anomaly; if minimizing the L1 norm of x is subject to $Ax = b$, there will be no solution.

IV. EXPERIMENTAL RESULTS

We conduct experiments on real trajectory data of taxicabs in Beijing to evaluate the effectiveness and efficiency of the proposed framework. The details of the datasets are as follows.

The Road network of Beijing contains 13,722 intersections and 79,258 road segments. The map is segmented into 238 regions using the high-level roads. Based on this partition, an abstract graph containing 238 nodes and 1,025 edges is formed.

The trajectory data is generated by approximately 30,000 taxicabs in Beijing over a period of four months (April, 2016 ~ October, 2016). The sampling interval is between 30s and 60s. For the real dataset, it is impossible to obtain sufficient ground truth of anomalies to evaluate the proposed method. Thus, we generate synthetic dataset based on real trajectory data. Specifically, we first partition one day into 144 time intervals and find the Origin-Destination (OD) node pairs that have more than five trips. In each interval, we assign a certain amount of simulated traffic on each OD pair. The most of OD pairs are assigned the normal traffic as presented in Fig. 7(a). To synthesize the first anomaly type, we randomly choose several OD pairs to assign traffic followed the distribution shown in (b); when synthesizing the second anomaly type, we manually cut off some links with great traffic in some time intervals, which may lead to rapidly increase of traffic on some alternative links of them, as presented in (c); to synthesize the third anomaly type, we modify the traffic assignment of a large proportion of OD-pairs in a certain day as (d) shown.

A. Efficiency

As the anomalous path inference mainly serves for offline review and analysis that does not refer to the efficiency as a major merit, we mainly evaluate the efficiency of SWTD through comparing SWTD with DTA and OTA [9]. Specifically, we first construct different scales networks with different number of links. Then we perform the three algorithms and report the relation between the time cost and the number of links (I_2) in Fig. 8(a). As an offline algorithm, the cost of OTA grows rapidly with the increase of I_2 ; while SWTD and DTA have a relatively low computational cost. By comparison, SWTD slightly outperforms DTA. Because DTA need to diagonalize the variance matrices $C_d \in \mathbb{R}^{I_d \times I_d}$ of mode- d unfolding of the tensor, despite it incrementally update the variance matrices; while SWTD construct a rank $R_d + 2$ matrix to approximate the unfolding matrix and diagonalize the smaller matrices ($R_d \ll I_d$). (b) shows the relation between the time cost and size of day dimension (I_3). DTA and SWTD remain basically constant. (c) shows the time cost as a function of the rank of unfolding matrix along the time mode (I_1). As (c) presented, the rank of matrix has a weaker impact on the efficiency of DTA and SWTD.

B. Effectiveness

Since the anomaly dataset is very imbalanced, we use the Precision-Recall (PR) metric [10] to evaluate the effectiveness of our method. And we compare our method with two baselines, DTA and PCA. Fig. 9 shows the PR curve of each method. The PR curve shows the tradeoff between precision and recall for

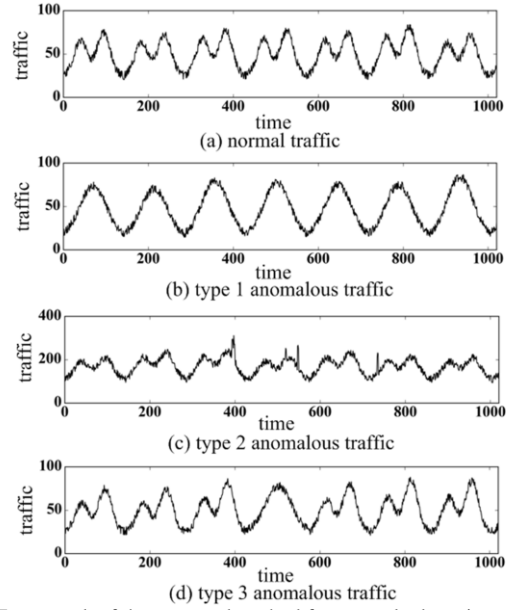


Fig. 7. Framework of the proposed method for anomaly detection

different threshold, and a large area under the curve represents both high recall and high precision of the algorithm. As Fig. 9 shown, STWD exhibits its advantages over PCA and DTA. Next, we investigate the anomalous path inference algorithm based only on sparsity maximization (SM), best matching (BM) and considering sparsity and flow simultaneously (SF). The paths accountable for the 1st and 3rd anomalous type can be directly obtained from the simulated network. Table 1 and Table 2 present the precision and recall of the two algorithms for the two types of anomalies, respectively. SF has a better performance than SM and BM. For the 2nd anomaly type, it is difficult to obtain the ground truth of the paths influenced by

TABLE I
THE PRECISION AND RECALL OF SM, BM AND SF ON THE 1ST TYPE OF ANOMALOUS PATH INFERENCE

Num. of paths	Num. of links	Precision			Recall		
		SM	BM	SF	SM	BM	SF
10	7	0.192	0.667	0.615	0.900	0.600	0.800
15	8	0.255	0.583	0.688	0.933	0.467	0.733
20	29	0.273	0.636	0.643	0.967	0.700	0.900
25	17	0.229	0.464	0.581	0.880	0.520	0.720
30	22	0.206	0.677	0.686	0.967	0.700	0.800

TABLE II
THE PRECISION AND RECALL OF SM AND SF ON THE 3RD TYPE OF ANOMALOUS PATH INFERENCE

Num. of paths	Num. of links	Precision			Recall		
		SM	BM	SF	SM	BM	SF
10	13	0.233	0.571	0.533	0.999	0.600	0.800
20	15	0.196	0.591	0.607	0.950	0.650	0.850
30	17	0.355	0.703	0.697	0.900	0.633	0.833
40	33	0.278	0.636	0.667	0.925	0.700	0.850
50	32	0.182	0.744	0.722	0.880	0.580	0.780

TABLE III
THE NUMBER AND FLOW OF ANOMALOUS PATH INFERRED BY SM AND SF ON THE 2ND TYPE

Num. of links	Num. of inferred paths			Ave. flow of inferred paths		
	SM	BM	SF	SM	BM	SF
3	45	14	22	22	47	83
7	84	23	30	16	28	75
12	105	27	36	31	89	95
16	116	31	45	26	14	80
18	131	46	62	24	31	73

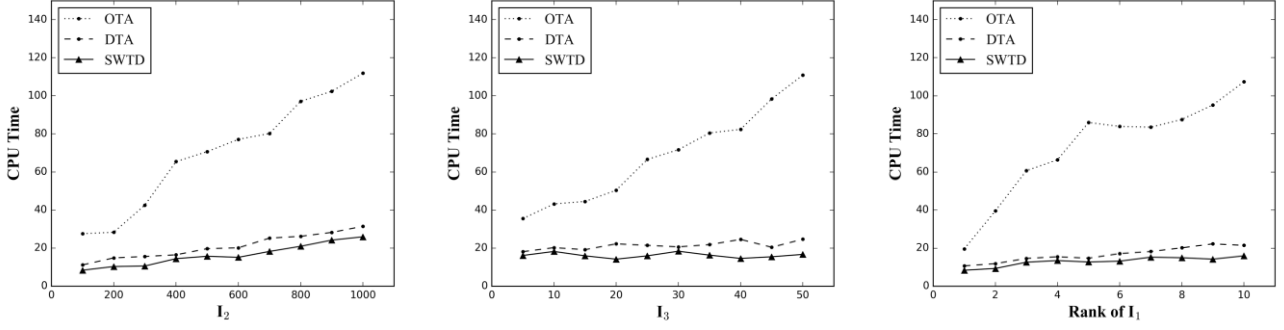


Fig. 8. The 3rd order sliding window tensor of traffic in the road network

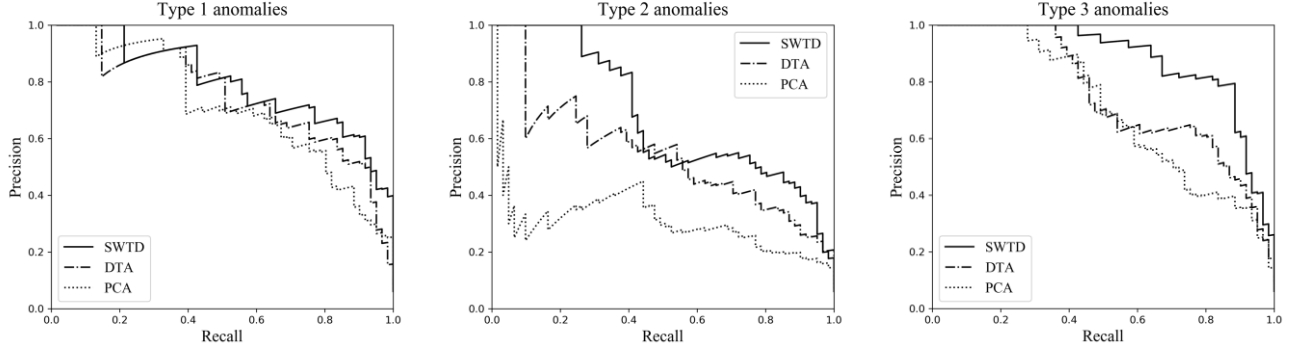


Fig. 9. The 3rd order sliding window tensor of traffic in the road network

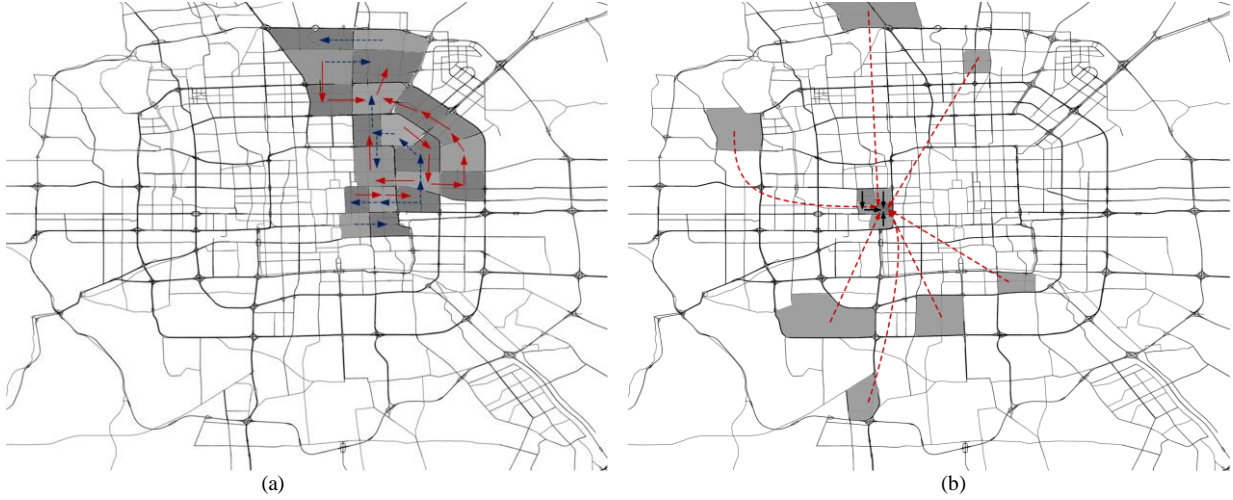


Fig. 10. The 3rd order sliding window tensor of traffic in the road network

the anomaly. Therefore, we investigate the number and average flow of inferred anomalous paths, as presented in Table 3. Compared with SM and BM, SF is more reasonable and offers a better understanding for anomalous events. However, BM is still a feasible method when the flows of paths are unknowable.

C. Real Case studies

Fig. 10 highlights two anomalous events that are discovered by the proposed methods from real trajectory dataset. The first anomalous event occurs during 9:30AM-4:00PM on 4/16/2017, as Fig. 10(a) presented. SWTD identify this anomaly as the 3rd type, for it breaks the short-time and spatial correlations simultaneously. If observing from the link perspective, we found that many links located in the northwest breaks their long-term correlation but has a short correlation. Specifically, the traffic of these links exhibits a great change, which is

similar to each other. The links with increased flow are marked with red solid arrows and the links with decreased flow are marked with blue dotted arrows. Through investigating the events reported by Beijing Transportation Bureau, we find that this anomaly refers to Beijing International Marathon in 2017. The race participated by more than 20,000 people passes through some main roads such as west ring roads etc., which generally coincide with the links marked by blue dotted arrows. To hold the race, a traffic control was enforced on its route and a large amount of vehicles have to detour, which result in the great flow on the links marked by red solid arrows.

Another case is presented in (b). The four anomalous links located near the center of the city occur in 9:20AM 10/21/2107. SWTD identifies the four links as the 2nd anomaly type, for they all break the short-term correlation and long-term correlation. Using the proposed path inference algorithm, we further find

seven anomalous OD-pairs marked by red dotted arrows; these OD-pairs have the common destination region near the anomalous links and their original regions are dispersed on the city map. The flows of these OD-pairs are slightly greater than ever before, and most of the links passed through by them still have the normal traffic. However, the confluences of these flows cause the links near the destination to be identified as anomalies. There is no record of these anomalies links in the event reports. Through Google Map, we find that the original regions are mainly residential areas or subway entrance, and their common destination is Beijing Children's Hospital. Therefore, we infer that this anomalous event may be caused by seasonal influenza.

V. RELATED WORK

In this section, we review two relevant research fields as follow

A. Anomaly detection in city-wide road networks

In recent work [11], GPS trajectory data of vehicles is used to discover the traffic jam. Chawla et al. [1] use PCA to detect anomalies based on taxi trajectories and then used a optimization technology to infer the anomalous paths by solving the L1 inverse problem. Pan et al. [12] first identify anomalous events according to the routing behavior of drivers, and then mine representative terms from social media to describe the detected anomalous events. Pang et al. [13,14] adapt likelihood ratio test statistic to rapidly detect anomalies based on GPS data. However, their method is not concerned with data sparsity that is widespread in real spatio-temporal data. To deal with this problem, Zheng et al. [15] propose a probability-based data fusion method to detected anomalies using dataset across different domains. In [16], Zheng et al. detect flawed planning of road networks using taxi trajectories. Liu et al. [17] construct causality trees to reveal intersections among spatio-temporal anomalies and potential flaws in the design of road networks. A common problem in the existing studies is that the diversity of spatio-temporal anomalies is not considered adequately.

B. Anomaly detection based on tensor

For data in many domains includes high dimensions structure, tensor factorization has been increasingly popular. Zhang et al. [18] proposed a tensor-based method to detect the targets in hyperspectral imagery data with both spectral anomaly and spatial anomaly characteristics. Shi et al. [20] represent spatio-temporal data stream generated from sensor networks as an incremental tensor and proposed incremental tensor decomposition for online anomaly detection. To detect the events in the traffic network, Fanaee-T and Gama [19] constructed a hybrid model from a topology tensor and a flow tensor, and then used a tucker decomposition technology with adjustable core size. However, these studies did not deal with the diversity of anomalies, while our methods focus on online detection of different types of anomalies in traffic network.

VI. CONCLUSION

In this paper, we propose a framework to detect multiple types of anomalies in road networks though mining from vehicle

trajectories. In this framework, we represent the network traffic as a tensor, and use a sliding window tensor factorization to capture the spatial and different scale temporal patterns with lower cost, then, we detect the different types of anomalies through measuring the deviation from different spatial or temporal patterns. Furthermore, we infer the anomalous paths according to the discovered anomalous links by combining the sparsity maximization and flows of paths. We conduct synthetic experiments and a case study based on a real-world trajectory dataset to evaluate the effectiveness and efficiency of the proposed methods. The experimental results demonstrate that the proposed methods can not only detect the different types of anomalies in city-wide road network, but also provide a better understanding of anomalies.

REFERENCES

- [1] S. Chawla, Y. Zheng and J. Hu, "Inferring the root cause in road traffic anomalies" in *Proc. ICDM*, Brussels, Belgium, 2012, pp. 141-150.
- [2] T. G. Kolda and B. W. Bader, "Tensor decompositions and applications". *SIAM review*, vol. 51, no. 3, pp. 455-500, 2009.
- [3] Y. Lou, C. Zhang, Y. Zheng et al., "Map-matching for low-sampling-rate GPS trajectories," in *Proc. GIS.*, Seattle, WA, USA, 2009, pp. 352-361.
- [4] N. J. Yuan, Y. Zheng and X. Xie, "Segmentation of urban areas using road networks," Microsoft Corp. Redmond, WA, USA, Tech. Rep. MSR-TR-2012-65, 2012.
- [5] T. M. Toolan and D. W. Tufts, "Improved fast adaptive subspace tracking," MIT Lincoln Lab., Lexington, MA, USA, Proj. Rep. ESC-TR-2005-071, Jan. 10, 2006.
- [6] A. Lakhina, M. Crovella and C. Diot, "Diagnosing network-wide traffic anomalies," in *Proc. SIGCOMM*, Portland, OR, USA, 2004, pp. 219-230.
- [7] Y. Zhang, Z. Ge, A. Greenberg et al., "Network anomography" In *Proc. SIGCOMM*, Philadelphia, PA, USA, 2005.
- [8] H. Kasai, W. Kellerer, M. Kleinstueber et al., "Network volume anomaly detection and identification in large-scale networks based on online time-structured traffic tensor tracking," *IEEE Transactions on Network and Service Management*, vol. 13, no. 3, pp. 636-650, 2016.
- [9] J. Sun, D. Tao, and C. Faloutsos, "Beyond streams and graphs: dynamic tensor analysis," In *Proc. KDD*, Philadelphia, PA, 2006, pp. 374-383.
- [10] T. Saito and M. Rehmsmeier, "The precision-recall plot is more informative than the ROC plot when evaluating binary classifiers on imbalanced datasets," *PloS one*, vol. 10, no. 3, e0118432, 2015.
- [11] W. Dong and A. Pentland, "A network analysis of road traffic with vehicle tracking data," In *Proc. AAAI*, Arlington, VA, USA, 2009, pp. 7-12.
- [12] B. Pan, Y. Zheng, D. Wilkie, et al., "Crowd sensing of traffic anomalies based on human mobility and social media," in *Proc. GIS.*, Orlando, FL, USA, 2013, pp. 344-353.
- [13] L. X. Pang, S. Chawla, W. Liu et al., "On detection of emerging anomalous traffic patterns using GPS data," *Data & Knowledge Engineering*, vol. 87, pp. 357-373, 2013.
- [14] M. Wu, X. Song, C. Jermaine et al., "A LRT framework for fast spatial anomaly detection," In *Proc. KDD*, Paris, France, 2009, pp. 887-896.
- [15] Y. Zheng, H. Zhang and Y. Yu, "Detecting collective anomalies from multiple spatio-temporal datasets across different domains," in *Proc. GIS*, Seattle, WA, USA, 2015.
- [16] Y. Zheng, Y. Liu, J. Yuan et al., "Urban computing with taxicabs," in *Proc. Ubicomp*, Beijing, China, 2011, pp. 89-98.
- [17] W. Liu, Y. Zheng, S. Chawla, "Discovering spatio-temporal causal interactions in traffic data streams," in *Proc. KDD*, San Diego, CA, USA, 2011, pp. 1010-1018.
- [18] X. Zhang, G. Wen, W. Dai, "A tensor decomposition-based anomaly detection algorithm for hyperspectral image," *IEEE Transactions on Geoscience and Remote Sensing*, vol. 54, no. 10, pp. 5801-5820, 2016.
- [19] H. Fanaee-T and J. Gama, "Event detection from traffic tensors: A hybrid model," *Neurocomputing*, vol. 203, pp. 22-33, 2016.
- [20] L. Shi, A. Gangopadhyay, V. P. Janeja, "STenSr: Spatio-temporal tensor streams for anomaly detection and pattern discovery," *Knowledge and Information Systems*, vol. 43, no. 2, pp. 333-353, 2015.